The function of mitogen activated protein kinases in zebrafish development

Krens, S.F.G.

V

ERK1 and ERK2 MAPK are key regulators of distinct target gene signature sets in zebrafish embryogenesis

S. F. Gabby Krens, Maximiliano Corredor-Adámez, Shuning He,
B. Ewa Snaar- Jagalska, Herman P. Spaink

submitted

Abstract

The MAPK signaling proteins are involved in all eukaryotic cellular processes and in signaling networks. However, specific function of most of these proteins in vertebrate development remain elusive because of potential redundancies. For instance, the upstream activation pathways for ERK1 and ERK2 are highly similar, and also many of their known downstream targets are common. In contrast, mice and zebrafish studies indicate distinct roles for both ERKs in cellular proliferation, oncogenic transformation and development. A major bottleneck for further studies is that relatively few i*n vivo* downstream targets of these kinases have been identified conclusively.

Microarray based gene expression profiling of ERK1 and ERK2 knockdown zebrafish embryos resulted in specific gene expression signature sets that showed pronounced differences in gene ontology analyses. Signaling pathways were analyzed for the BMP, FGF, Nodal and Wnt signaling pathways that are important for embryogenesis. Specific effects of ERK1 and ERK2 knockdown treatments were confirmed by whole mount in situ hybridization experiments.

The gene ontology analyses showed that ERK1 and ERK2 have specific roles in embryogenesis and target distinct gene sets involved in vertebrate development, confirming the embryonic knockdown phenotypes. For ERK1 we identified a connection with genes involved in dorsal-ventral patterning and subsequent embryonic cell migration. For ERK2 we identified a connection with genes involved in cell-migration, mesendoderm differentiation and patterning. The outcome of the predictions for ERK2 knockdown on developmental signaling were confirmed by the observed effects on mesoderm and endoderm patterning and subsequent whole mount in situ hybridization experiments.

Introduction

ERK1 and ERK2 (Extra-cellular signal Regulated protein Kinases) are most likely the best studied members of the mitogen activated protein kinase (MAPK) proteins. Despite efforts and their biological - medical importance, still relatively few *in vivo* downstream targets of these kinases have been identified conclusively, especially when considering the numerous cellular events and signaling networks they are involved in (Johnson et al., 2005). Most of the target proteins and downstream genes have been identified by *in vitro* studies using cell culture systems.

Specific roles for both ERKs are described for cellular proliferation, as mouse embryos fibroblasts (MEF) isolated from *erk1*-/- mice grew faster

than wild type cells. The tumorigenicity of transplanted NIH 3T3 cells stably expressing an oncogenic form of Ras in nude mice was largely inhibited by co-transfection of ERK1, but not by ERK2 or p38 (Vantaggiato et al., 2006). In diseases ERK1 and ERK2 can display distinct cellular functions, as have been shown for the formation of cancer (Lloyd et al., 2006). In addition, divergent roles for ERK1 and ERK2 were already shown by the different effect of the knockout studies performed in mice as *erk1*-/- mice are viable and fertile (Pagès et al.1999), while *erk2*-/- mice die *in utero* before embryonic day (E) 8.5 (Saba-El-Lei et al., 2003).

To study and compare the developmental roles of ERK1 and ERK2 we used specific morpholino antisense oligonucleotides (MO), to block translation of ERK1 and ERK2. We previously showed that mild knockdown of ERK1 or ERK2 differentially affected convergence extension movements, but did not disturb patterning of the embryo. Stronger knockdown conditions of ERK2 led to a more severe phenotype, as ERK2MO morphants did not go into epiboly, whereas ERK1MO morphants still developed further and entered gastrulation stages. In addition, immuno-histochemical studies showed that ERK phosphorylation was completely abolished in the blastula margin of ERK2 morphants, indicating that ERK2 is the active ERK MAPK in the margin and essential for epiboly initiation and further progression of the developmental program (chapter 4, this thesis). Possibly ERK2 also functions in mesendodermal differentiation processes in the blastula margin, as FGF is known to activate the canonical MAPK pathway in a Ras dependent manner (Gotoh and Nishida, 1996; Bottcher and Niehrs, 2005). The severe phenotype that we observed upon ERK2 knockdown in zebrafish embryos indicate that ERK2 has a more dominant role during early developmental processes, as also suggested by the mice knockout phenotypes.

Here we aim to further determine specific downstream gene targets of ERK1 and ERK2 during vertebrate development, by performing expression profiling analysis using a microarray approach. We compared the expression profiles of ERK1 and ERK2 knockdown embryos, using specific morpholino antisense oligonucleotides (MO), which specifically block the translation of a gene of interest into a functional protein (Nasevicius and Ekker, 2000).

Microarray technology enables gene characterization based on systematic and comprehensive expression studies of large sets of genes. In addition, the availability of the zebrafish genome sequence and the annotation of all predicted genes help us to understand the link between genes and their functions. Newly developed software programs and web-based analysis tools, e.g. Rosetta Resolver, GenMAPP and GeneTOOLS eGOn, are helpful for the processing and comparisons of large expression datasets and biological in-

terpretation of the data. For instance, these tools facilitate the prediction of interconnection between developmental signaling pathways that can be tested by biological assays.

Analysis of the obtained data revealed that ERK1MO and ERK2MO knockdown affect signature sets of common target genes, as well as signatures sets of specific genes. Surprisingly, we also identified gene sets in which the expression patterns were anti-correlated. Several signature marker genes identified in this study were confirmed by quantitative real time PCR and in situ hybridization. We performed signaling pathway analysis on the obtained ERK1 and ERK2 transcriptome signatures, using the GenMAPP software program (Dahlquist et al., 2002) for the analysis of important signaling cascades during early vertebrate development. These include BMP, FGF, Nodal and Wnt signaling pathways (Schier and Talbot, 2005). For ERK1 knockdown we identified a connection with genes involved in dorsal-ventral patterning and subsequent embryonic cell migration. For ERK2 knockdown we identified a connection with genes involved in mesoderm and endoderm initiation, differentiation and patterning. Many of these genes also play a role in morphogenic cell migration processes during later stages of development. The outcomes of the predictions for ERK2 knockdown on developmental signaling were confirmed by the observed effects on mesoderm and endoderm induction and subsequent whole mount in situ hybridization experiments.

Results and discussion

Distinct gene expression signature sets of ERK1 and ERK2 knockdown embryos

A morpholino knockdown approach was used to block translation of either ERK1 or ERK2 by injection of 0.4mM (=3.4 ng/embryo) morpholinos (MO) targeting ERK1 (ERK1MO) or ERK2 (ERK2MO). The knockdown embryos, also referred to as morphants, showed severe phenotypes after depletion of ERK2. These embryos did not enter epiboly at 4.5 hpf and the blastula cells remained on top of the yolk, preventing further development of the embryo (Fig.1C). Wild type embryos reached 30% epiboly at this time (Fig.1A) (Kimmel et al., 1995). In contrast, ERK1 morphants did not show any obvious phenotypes at this point, and had entered epiboly (Fig.1B). The severe phenotypes of ERK2 morphants indicate defects in crucial early developmental processes and it is likely that the expression of a significant number of genes has changed.

To identify specific gene pools affected by the knockdown of ERK1 or ERK2,

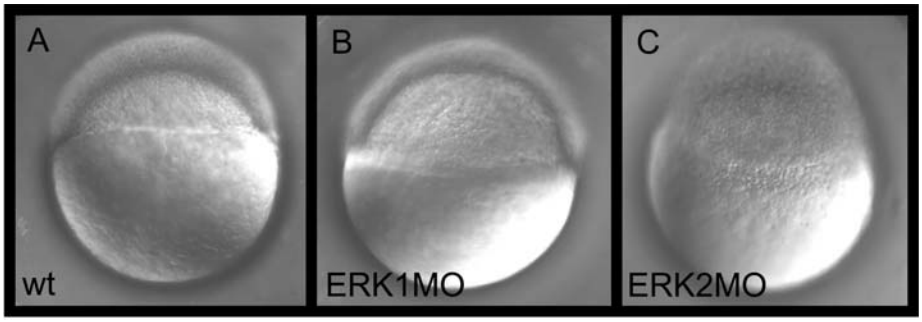

Figure 1. Differential Interference Contrast (DIC) microscopy images of 4.5h old embryos. Wildtype (wt) and ERK1MO morphants are at approximately 30% epiboly stage and undergo epiboly, whereas ERK2 morphants do not initiate epiboly.

and to identify possible downstream targets, microarray based transcriptome analysis was performed using Agilent zebrafish microarrays. Total RNA was isolated from the morpholino injected embryos at 30% epiboly time point. As a control for general morpholino effects, a standard control morpholino (GeneTools Philomath, OR, USA) was injected in the same concentration. This did not result in any phenotypes during zebrafish development. Still, injection of standard control MO could have specifically affected the transcriptome of the developing embryos. Therefore, we also performed microarray analysis comparing standard control MO to embryos injected only with MO injection-buffer (1× Danieau's buffer, containing 1% Phenol red solution). The obtained standard control MO signature set consists of 574 probes that showed a significant (combined p-value smaller than 10^{-5}) change in their expression by injection of the standard control MO at 30% epiboly. Of this signature set only 26 genes were common with both the ERK1 and ERK2 knockdown expression signature sets (Table S7; online supplementary data at http://biology.leidenuniv.nl/~krens). Since in these comparisons use was made of ratios against the standard control MO, we can conclude that the expression of this overlap gene set is specifically affected by the standard control MO. Therefore, this set of 26 genes was flagged as putative false positives in further microarray analyses. The remainder of the 574 set of probes, most likely influenced by aspecific effects of morpholino injections, will be compensated for by using ratios against standard control MO in all ERK1 and ER2 analyses.

The RNA from standard control MO injected embryos was used as a reference also in dye swaps to compare the transcriptomes of both ERK1MO and ERK2MO injected embryos. Comparison of the gene expression profiles of ERK1 and ERK2 morphants at 30% epiboly showed a larger number of probes with significant changes ($p<10^{-5}$) in ERK2 than in ERK1 morphants,

as illustrated in a Venn-diagram (Fig.2A). Furthermore, the number of probes with an altered expression was larger and with a higher fold of change in expression for ERK2 then for ERK1 morphants (Fig.3). This is in agreement with the phenotype of ERK2 knockdown embryos that indicates a more prominent role for ERK2 in early development. (Fig.1). The probes that were found also to be effected by the standard control MO (less than 1% of the total number affected genes), were marked with an asterisk (*) in the annotated gene-tables for ERK1 and ERK2 knockdown (Table S1-S6; online supplementary data at http://biology.leidenuniv.nl/~krens). Several genes are represented by multiple

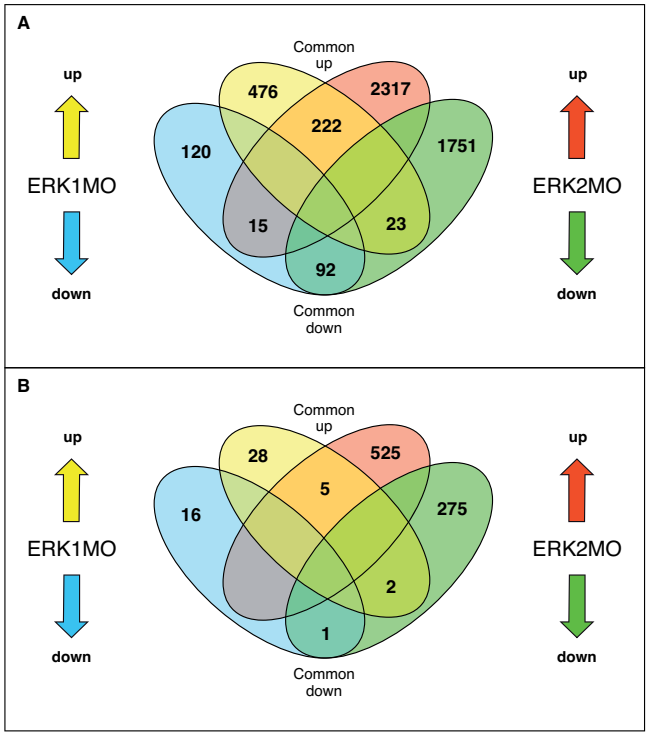

Figure 2. Venn-diagram comparison of the ERK1 and ERK2 knockdown expression profiles at 30% epiboly stage. The Venn diagram was constructed twice, with the complete signatures (A) and with the stringent signatures (B). The signatures of ERK1 and ERK2 morphants are split in up and down regulated, therefore the Venn diagram shows the numbers of specifically up and down regulated genes, common up and down regulated genes, and two anti-correlated gene pools (up regulated in ERK1MO – down regulated in ERK2MO and down regulated in ERK1MO – up regulated in ERK2MO); yellow = up-regulated by ERK1MO (ratio > 1), blue = down-regulated by ERK1MO (ratio <1), red = up-regulated by ERK2MO (ratio > 1), green = down-regulated by ERK2MO (ratio <1).

probes on the microarray slides and therefore the same gene occurs several times in the annotated tables. Observations such as this give additional support for the obtained gene expression signatures and confirm that the expression of these genes is affected by ERK1 or ERK2 knockdown.

The result show that different probes were specifically regulated by either knockdown of ERK1 (476 probes up-regulated, 120 probes down-regulated) or knockdown of ERK2 (2317 probes up-regulated, 1751 probes down-regulated). Furthermore, a number of 222 probes were commonly up-regulated, 92 probes are commonly down-regulated. Maybe even more interesting are the probes which were regulated in an anti-correlated manner: 23 probes were up-regulated by knockdown of ERK1 whereas they were down-regulated by knockdown of ERK2 (anti-correlated gene-pool 1) and 15 probes were down-regulated by knockdown of ERK1 whereas they were up-regulated by knockdown of ERK2 (anti-correlated gene-pool 2). The commonly and anti-correlated regulated

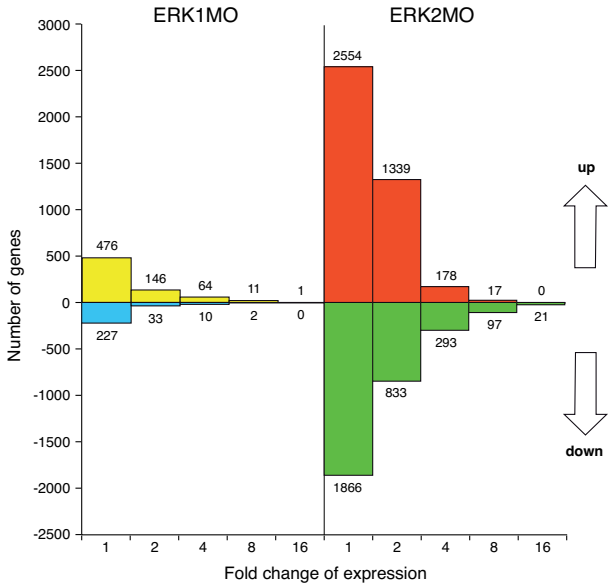

Figure 3. Knockdown of ERK2 affects the expression of more genes, and with a higher fold of changes than knockdown of ERK1. The graph represents the total number of genes that showed changes in expression, as well as their fold of change (greater than 1, 2, 4, 8, and 16 fold changes) upon knockdown of ERK1 or ERK2 at 30% epiboly ($p<10^{-5}$). The number of genes with changed expression levels and the fold of change after knockdown of ERK1 were lower than upon ERK2 knockdown.

probes have been annotated and are listed in tables S1 to S4 and assigned gene designations. To identify the ERK1MO and ERK2MO specific genes, we focused on the probes that were most significantly affected. Therefore we used the following criteria: the absolute fold change must be at least 1.5 in each independent replicate and the common p-value provided by the error-model taking into account all hybridizations must be smaller than 10^{-5} to compensate for multiple testing false positives. These probes are also depicted in a Venn-diagram (Fig.2B). The stringent selected probes that were only found in either ERK1MO or ERK2MO gene-pools were manually annotated and assigned gene designations as listed in table S5 and S6.

Quantitative real-time PCR analyses confirm the different ERK1MO and ERK2MO gene expression profiles

To confirm the obtained gene expression profiling by the microarrays experiments, quantitative real-time PCR (qPCR) analysis was performed on three differentially regulated genes. The expression level were tested on the same RNA samples as used for the microarray analysis for *mycn* (v-myc, myelocytomatosis viral related oncogene, neuroblastoma derived, NM_212614), *fos* (FBJ murine osteosarcoma viral oncogene homolog, NM_205569) and *mos* (moloney murine sarcoma viral oncogene homolog, NM_205580) (Fig.4). β-actin was taken as reference to compare the expression levels of the selected genes in ERK1MO, ERK2MO and standard control MO injected embryos. The qPCR expression levels for *fos*, *mos* and *mycn* in ERK1MO or ERK2MO were compared to standard control MO injected embryos, in the same way as was performed for the microarray analysis. The obtained qPCR data for the expression of *fos* showed an anti-correlated regulation comparing ERK1 and ERK2 knockdown to standard control MO conditions. *Fos* is down-regulated by knockdown of ERK1 and up-regulated by knockdown of ERK2, compared to the expression-level of *fos* in standard control MO (Fig.4A). The expression level of *mos* is up-regulated, whereas *mycn* is down-regulated in both ERK1MO and ERK2MO conditions, compared to the standard control MO (Fig. 4B and C respectively).

The data obtained by qPCR and microarray experiments for the expression-levels of *fos*, *mos* and *mycn* in ERK1MO and ERK2MO were compared to the expression levels of these genes in the standard control MO injected embryos (Fig.4D). The qPCR data confirmed the change in expression levels of the selected genes as observed by microarray analysis, and thus the unique gene expression profiles for ERK1MO and ERK2MO mediated knockdown in early zebrafish development (30% epiboly).

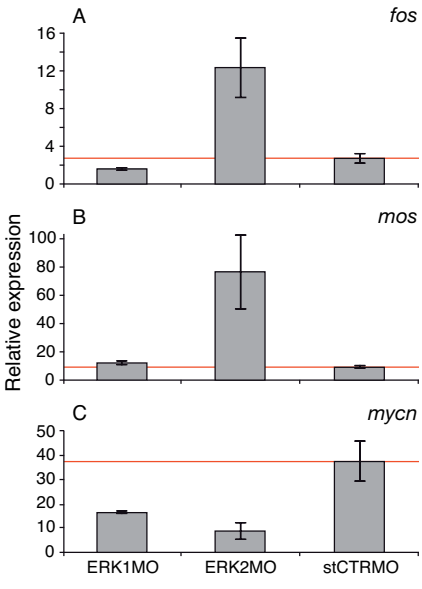

D

Gene	morpholino	qPCR	Agilent 22K	
fos	ERK1MO	-1.92	-1.46	⇩
	ERK2MO	4.50	2.31	⇧
mos	ERK1MO	1.37	3.44	⇧
	ERK2MO	8.87	10.35	⇧
mycn	ERK1MO	-2.22	-1.71	⇩
	ERK2MO	-4.35	-5.37	⇩

Figure 4. Quantitative real-time PCR confirmation of the microarray results. (A-C) qPCR was performed on three genes that showed differential regulation of expression in response to knockdown to either ERK1, ERK2 and the standard control MO control: *fos* (NM_205569, down in ERK1MO, up in ERK2MO), *mos* (NM_205580, up in both ERK1MO and ERK2MO), *mycn* (NM_212614 down in both ERK1MO and ERK2MO), correlated to the β-actin housekeeping gene. The fold of changes of these genes, detected by qPCR assay and microarray, are listed in a table (D). ⇧ = induction of expression, ⇩ = repression of expression, compared to the standard control MO.

Gene Ontology (GO) analysis

The gene expression signatures of the ERK1 and ERK2 morphants were used to perform gene ontology analysis. Gene ontology consists of three structured controlled vocabularies (ontologies) that describe genes and gene-function (http://www.geneontology.org) and each gene ontology has a unique nu-

merical identifier. The GO-clusters are structured in a tree, which can be queried at different levels. This allows us to assign properties from genes at different levels, depending on the depth of knowledge or interest concerning the genes of interest. Gene ontologies describe gene products in terms of their associated 'biological processes' (GO:0008150), 'cellular components' (GO:0005575) and 'molecular functions' (GO:0003674) in a species-independent manner. To do so, we first annotated the complete Agilent 22K-zebrafish microarray chip by BLAST searches with all oligonucleotide sequences in the zebrafish genome. From the complete number of 21506 oligonucleotides from the Agilent 22K zebrafish chip, 21485 oligonucleotides were assigned an Unigene ID according to the highest similarity. Next, the Unigene ID-linked signature sets for ERK1 and ERK2 knockdown, were uploaded into the GeneTools eGOn V2.0 web-based gene ontology analysis software (explore Gene Ontology, database build #97) (Beisvag et al., 2006). These signature sets comprised 575 Unigene IDs in the case of ERK1 morphants and 2987 Unigene IDs in the case of ERK2 morphants were compared to the complete set of 21485 Unigene IDs from the Agilent 22K zebrafish microarray chip ('biological process'; 6036 Unigene IDs, 'molecular function'; 6322 Unigene IDs and 'cellular component'; 5606 Unigene IDs). As a result we were able to determine which gene ontology clusters were significantly over- or under represented in the ERK1MO and ERK2MO Unigene ID linked signature sets (Fig.5; p-values smaller than 0.05 are indicated with asterisk, p-values smaller than 0.02 are indicated with double asterisk). Several GO-clusters shared high similarity and were identified by similar groups of genes. We reduced the number of terms by excluding these overlapping GO-clusters. To ensure statistical relevance, also the GO-clusters that contained less than 10 Unigene IDs were removed. For the selected GO-terms, we calculated the relative fold of enrichment within the ERK1- and ERK2-morphant signature sets (Fig.5). The results showed a significant relative over- or under-representation of the number of Unigene IDs in ERK1 versus ERK2 morphants within the GO categories. For ERK1 versus ERK2 knockdown signature sets we obtained 5 or 14 GO-terms associated with 'biological processes' (Fig.5A), 3 or 16 associated with 'molecular functions' (Fig.5B) and 3 or 8 associated with 'cellular components' (Fig.5C), respectively.

Comparing the ERK1 and ERK2 knockdown signature sets some of these GO-terms show striking over- or under-representations in the number of representing Unigene IDs. For example, both the GO-terms 'cell cycle' (GO:0007049) and 'apoptosis' (GO:0006915) are significantly enriched upon ERK2 knockdown. When looking at the gene-lists in more detail (also using GenMAPP analysis, data not shown) inhibitory factors of apoptosis are down-regulated, whereas positive regulators of cell cycle were up-regulated. 'Cell

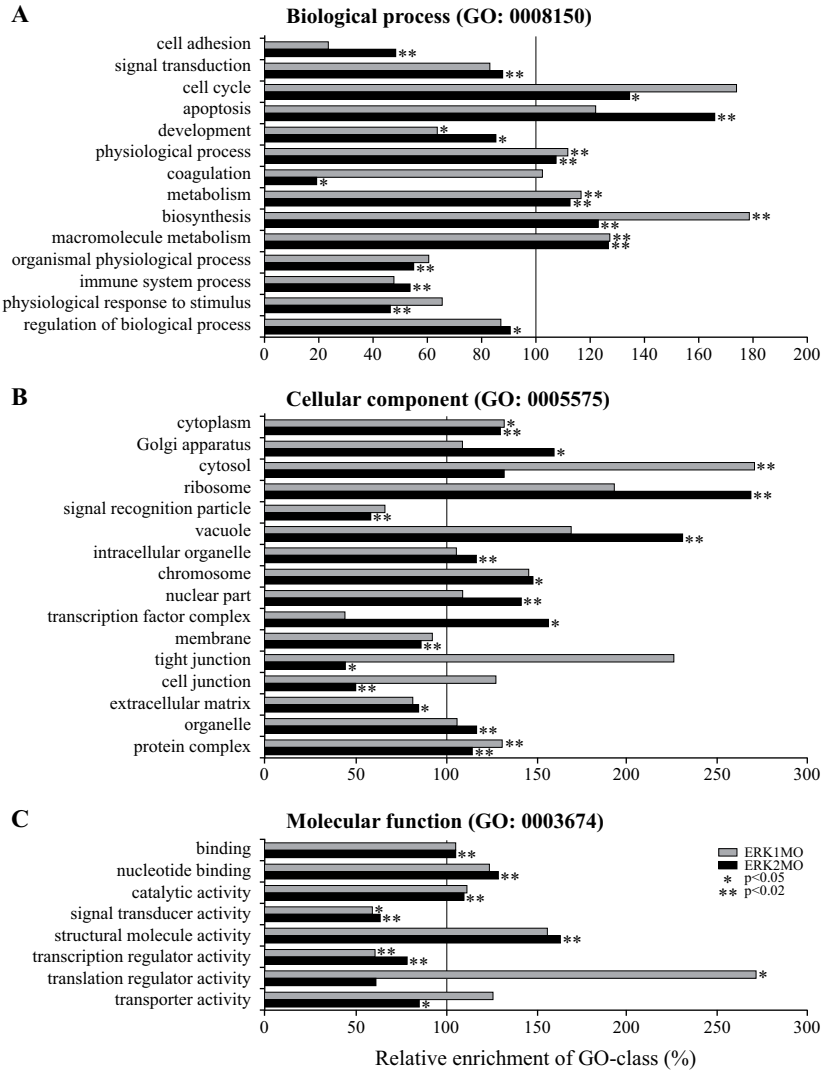

Figure 5. Statistical comparison of the Gene-Ontology distribution within the gene expression profiles, in ERK1 versus ERK2 knockdown embryos. (A) Biological process (GO:0008150), (B) Cellular component (GO:0005575) and (C) Molecular function (GO:0003674). ERK1MO and ERK2MO gene expression profiles were split in up- (red) and down- (green) regulated gene expression profiles and compared to the whole 22K Agilent chip, based on the Unigene-ID identifiers. The graph depicts the relative fold of enrichment (x-axis) of the statistically selected GO-clusters (y-axis), within one of the gene-pools: ERK1MO-up, ERK1MO-down, ERK2MO-up and ERK2MO-down (* = P<0.05, ** = P<0.01). Values greater than 1 were considered over-represented, values less than1 are considered as under-represented.

adhesion' (GO:0007155) and the cellular component GO-terms 'tight junction' and 'cell junctions' are significantly under-represented in the signature set of ERK2 morphants. Regulation of cell adhesion and the organization of tight- and cell-junctions are crucial for cell migration processes. Therefore these findings corroborate the crucial function of ERK2 in developmental cell migrations processes, as previously described in chapter 4.

Specifically for ERK1 knockdown a significantly enrichment of the 'translator regulator activity' (GO:0030528) GO-cluster was found. In contrast, the relative enrichment of this GO term in ERK2 morphants showed an underrepresentation. A significant overrepresentation of the GO term biosynthesis in ERK1 morphants correlates with these observations.

Interestingly, the GO-enrichment analysis showed that the number of genes within the GO-cluster 'development' (GO:0007275) were significantly underrepresented for both ERK1 (19 genes) and ERK2 (136 genes) morphants. This gives further support for the notion that both ERK1 and ERK2 have an important function during embryogenesis. From the 19 development-related genes whose expression was affected by ERK1 knockdown, 12 genes (63%) were not found in the ERK2 knockdown signature set. This shows that ERK1 and ERK2 have specific roles in embryogenesis and target distinct genes during vertebrate development, confirming the embryonic knockdown phenotypes.

Pathway Analysis of ERK1MO and ERK2MO mediated knockdown expression profiles

To further analyze putative down stream targets of ERK1 and ERK2 involved in early development, we focused on essential signaling pathways that are involved in early embryonic differentiation and patterning; Nodal, FGF, WNT and BMP- signaling pathways (Fig.8). For our study, we used the signaling pathway analyzing software program, GenMAPP (Gene Microarray Pathway Profiler, www.GenMAPP.org) (Dahlquist et al., 2002). This program is designed for viewing and analyzing gene expression data in the context of biological pathways and allows microarray-mediated gene expression signature sets to be displayed on biological (signaling) pathways. To do so, we first constructed *in silico* GenMAPP pathways for the zebrafish Nodal, FGF, (canonical) WNT and BMP signaling pathways (Fig.6). The construction of these GenMAPP signaling pathways is based on what is described in literature for zebrafish development, supported by the described knowledge for other vertebrate signaling processes and canonical signaling models, found on the Science's STKE Connections Map Database (http://stke.sciencemag.

org/cm/). Although it is clear that the Nodal, FGF, Wnt and BMP pathways are all interconnected, resulting in a complex signaling network, we performed a pathway-based analysis focusing on separate signaling pathways since the ways these signaling pathways exactly interconnect on a molecular scale is hardly understood yet.

The Unigene ID linked ERK1MO and ERK2MO signature sets that were used for GenMAPP analysis were not limited by fold change but instead we used all genes that had a combined p-value smaller than 10^{-5}. As previously mentioned, the number of genes that showed a changed expression in ERK2MO compared to ERK1MO injected embryos was far larger. Therefore, as expected, more genes with changed expression levels were found in the *in silico* GenMAPPs signaling pathways for ERK2MO, than for ERK1MO.

Knockdown of ERK1 did show only one gene (*smurf1*) with a significantly changed expression level within our BMP signaling GenMAPP. However, more genes were affected in FGF signaling: *fgf17b* (-1.4 fold) the MAPKKK *mos*, (+3.5 fold), transcription factor *cmyc* (-1.7 fold) and *srf* (serum response factor, -1.4 fold) showed significant changes in expression. In the Nodal pathway, the Nodal antagonist *lft1*/*antivin1* (+2.6 fold) and the EGF-CFC co-receptor *oep* (*one eyed pinhead*, -1.5 fold) were the only components found to be affected in ERK1 morphants. Furthermore, the ventrally expressed Wnt8-mediated organizer inhibitory gene *vent* (Melby et al., 2000) was down-regulated (-1.5 fold, Fig.6). Other genes involved in Wnt-signaling affected by ERK1 knockdown were *dab2* (disabled homolog 2, +1.5 fold), *ck2b* (casein kinase II beta subunit, -1.2 fold) and *ppp2r5e1* (Protein phosphatase 2A, regulatory B subunit, B56, +1.3 fold). These genes are also considered to be involved in early embryonic pattering pathways. Two genes involved in regulating gastrulation cell migration, *oep* and *quattro* (Warga and Kane, 2003; Dagget et al., 2004), were altered in expression.

The effect of depletion of ERK2 was far more severe in most of the analyzed signaling processes (Fig.6A-C). Key components of the FGF-pathway (*fgf8*, *fgfr4, frs2*, *bRaf*, *aRaf* and *mek1l*) and downstream target genes (*erm*, *eve1*, *pea*, *mkp3*, *spry2*, *ntl*, *spt*/*tbx16* and *tbx6*) were down-regulated, indicating already a block of the FGF-ERK pathway by ERK2 knockdown. Expression of some of these (mesoderm) target genes is initiated by Nodal. The Nodal-genes like *boz*/*dharma*, *squint*/*ndr1* and *smad2* are up-regulated, whereas inhibiting genes *lefty1* (*lft1*, -6 fold) and the ventral genes *vox* (-2 fold) and *ved* (-4 fold) are down-regulated in ERK2 morphants. Other nodal signaling mediator genes that are down-regulated are *oep* (-4 fold), *p300* (-2 fold), *foxh1*/*sur* (*schmalspur*, -2 fold) and the negative regulator of TGFβ signaling *TGIF* (-2 fold). The nodal-mediated endoderm gene *sox32*/*casanova*, expressed in the

margin, was down-regulated (-6 fold), and also the downstream target-gene *axial*/*foxA2* (-2 and -4 fold). Interestingly, *squint*/*ndr1* also functions as a positive regulation of fibroblast growth factor receptor signaling pathway (Maegawa et al.,2006).

The Wnt ligand *Wnt11* and receptors (*frz7a*, *7b*, *8a*, *9* and *10*) and the central mediator β-*catenin1* were down-regulated in ERK2 morphants, suggesting a severe inhibitory effect or even complete block of these pathways at this level. This inhibition of the Wnt pathway is also supported by the up-regulation of *axin2*/*conductin*, a scaffold protein from the β-catenin destruction complex, responsible for the degradation of β-catenin (Behrens et al., 1998). Down-regulation of the putative Wnt-target genes *vox*, *vent*, but also *otx2*, *sp5*, and *lim1* further support impaired Wnt-signaling. However, ERK2 knockdown also led to the down-regulation of the inhibitors *dkk1* and *sfrp1*, and up-regulation of the intracellular Wnt-signaling components *fxd8c*, *dab2*, β-*catenin2* and *tcf1*.

The effect of ERK2 knockdown on BMP signaling is also complex, as *bmp4* is up-regulated whereas *bmp1a*/*tolloid* and *bmp6* are down-regulated. This opposing effect is also found in the BMP antagonists, as *chordin* (*chd*) and the ventrally expressed membrane bound bmp-inhibitor *bambi* were down-regulated, whereas a different BMP antagonist *gremlin* is up-regulated. Adding to this complexity is the fact that the agonist *twisted gastrulation* (*twsg1a*) is up-regulated. The results clearly show that that dorsal-ventral patterning and also mesoderm patterning is severely affected but it is difficult to speculate about the downstream effects of all these changes of expression in the BMP pathway.

To confirm predicted effects of the Genmapp pathway analysis experimentally, we performed whole mount in situ hybridization on ERK1 and ERK2 morphants at 30% epiboly with marker genes regulated by Nodal, BMP, Wnt and FGF (Fig.7, Fig.8). This technique not only indicates the level of expression of a certain gene, but importantly also shows the localization of its expression. Different components of the Wnt / β−catenin pathway showed lower expression levels in ERK2 morphants. We showed that *goosecoid* (*gsc*) (Stachel et al., 1993), a downstream marker gene for the Wnt pathway at early developmental stages (Fig.7A-C) is not expressed in the ERK2 morphants. Knockdown of ERK1 did lead to a significant effect on the expression of *gsc*, but after knockdown of ERK2 no expression of *gsc* was detected by whole mount in situ hybridization. This confirms that canonical Wnt signaling was severely affected in ERK2 morphants, preventing subsequent expression of the Wnt-target gene *gsc*.

The *lefty 1* (*lft1* / *antivin1*) gene is a member of the TGF-beta superfamily that regulates left-right axis formation during embryogenesis via antagonistic activ-

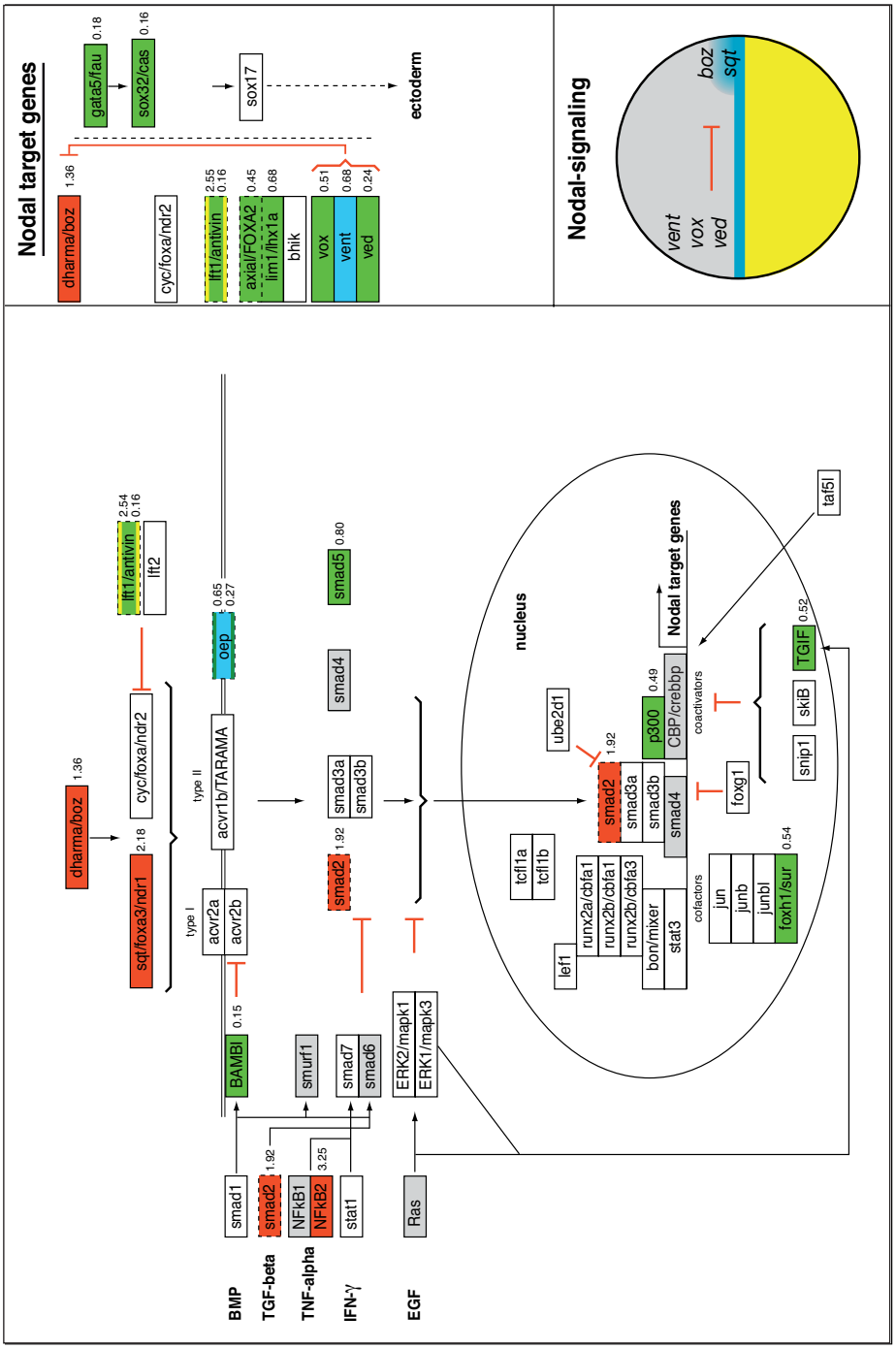
Nodal target genes
dharma/boz
1.36
gata5/fau
0.18
sox32/cas
0.16
sox17
ectoderm
cyc/foxa/ndr2
lft1/antivin
2.55
0.16
axial/FOXA2
lim1/lhx1a
0.45
0.68
bhk
vox
0.51
vent
0.68
ved
0.24
Nodal-signaling
vent
vox
ved
boz
sqt
dharma/boz
1.36
sqt/foxa3/ndr1
2.18
cyc/foxa/ndr2
lft1/antivin
2.54
0.16
lft2
type I
type II
acvr2a
acvr2b
acvr1b/TARAMA
oep
0.65
0.27
BAMBI
0.15
smurf1
smad7
smad6
smad1
smad2
1.92
NFkB1
NFkB2
3.25
stat1
ERK2/mapk1
ERK1/mapk3
Ras
smad2
1.92
smad3a
smad3b
smad4
smad5
0.80
BMP
TGF-beta
TNF-alpha
IFN-γ
EGF
nucleus
tcfl1a
tcfl1b
lef1
runx2a/cbfa1
runx2b/cbfa1
runx2b/cbfa3
bon/mixer
stat3
cofactors
ube2d1
smad2
1.92
smad3a
smad3b
smad4
p300
0.49
CBP/crebbp
coactivators
Nodal target genes
foxg1
jun
junb
junbl
foxh1/sur
0.54
snip1
skiB
TGIF
0.52
taf5l

Figure 6A

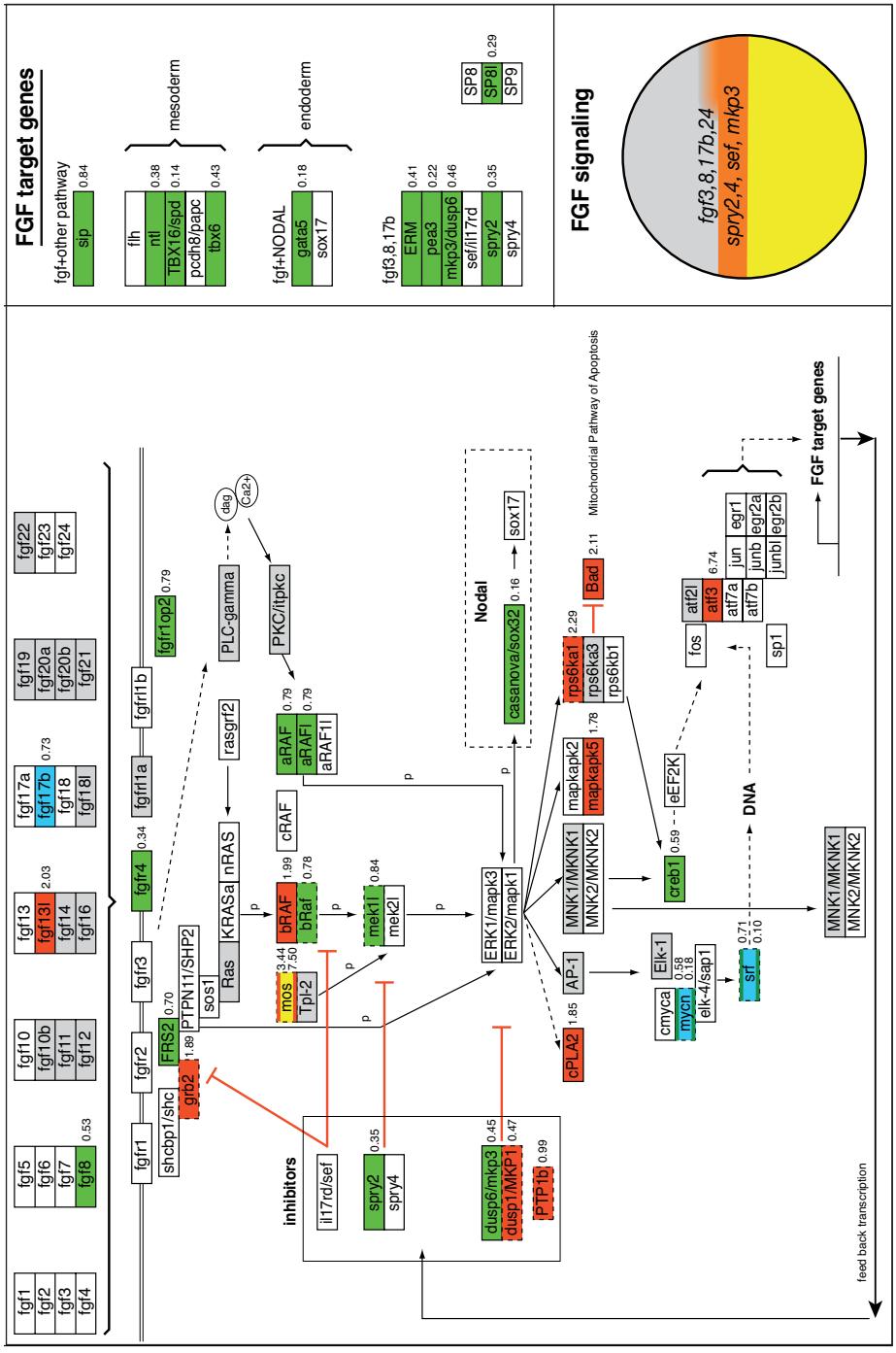
FGF target genes
fgf+other pathway
sip
0.84
fgf+NODAL
gata5
sox17
0.18
fgf3,8,17b
ERM
pea3
mkp3/dusp6
sef/il17rd
spry2
spry4
0.41
0.22
0.46
0.35
fgf1
fgf2
fgf3
fgf4
fgf5
fgf6
fgf7
fgf8
0.53
fgf10
fgf10b
fgf11
fgf12
fgf13
fgf13l
fgf14
fgf16
2.03
fgf17a
fgf17b
fgf18
fgf18l
0.73
fgf19
fgf20a
fgf20b
fgf21
fgf22
fgf23
fgf24
fgfr1
fgfr2
fgfr3
fgfr4
0.34
fgfrl1a
fgfrl1b
fgfr1op2
0.79
shcbp1/shc
grb2
1.89
FRS2
0.70
PTPN11/SHP2
sos1
Ras
KRASa
nRAS
rasgrf2
PLC-gamma
dag
Ca2+
PKC/itpkc
cRAF
aRAF
aRAFl
aRAF1l
0.79
0.79
bRAF
bRaf
1.99
0.78
mos
3.44
7.50
Tpl-2
mek1l
mek2l
0.84
ERK1/mapk3
ERK2/mapk1
Nodal
casanova/sox32
0.16
sox17
MNK1/MKNK1
MNK2/MKNK2
mapkapk2
mapkapk5
1.78
rps6ka1
rps6ka3
rps6kb1
2.29
Bad
2.11
Mitochondrial Pathway of Apoptosis
AP-1
cPLA2
1.85
Elk-1
0.58
cmyca
mycn
0.18
elk-4/sap1
creb1
0.59
eEF2K
fos
atf2l
atf3
6.74
atf7a
atf7b
jun
junb
junbl
egr1
egr2a
egr2b
sp1
DNA
srf
0.71
0.10
inhibitors
il17rd/sef
spry2
0.35
spry4
dusp6/mkp3
0.45
dusp1/MKP1
0.47
PTP1b
0.99
feed back transcription
FGF target genes
FGF signaling
fgf3,8,17b,24
spry2,4, sef, mkp3

Figure 6B

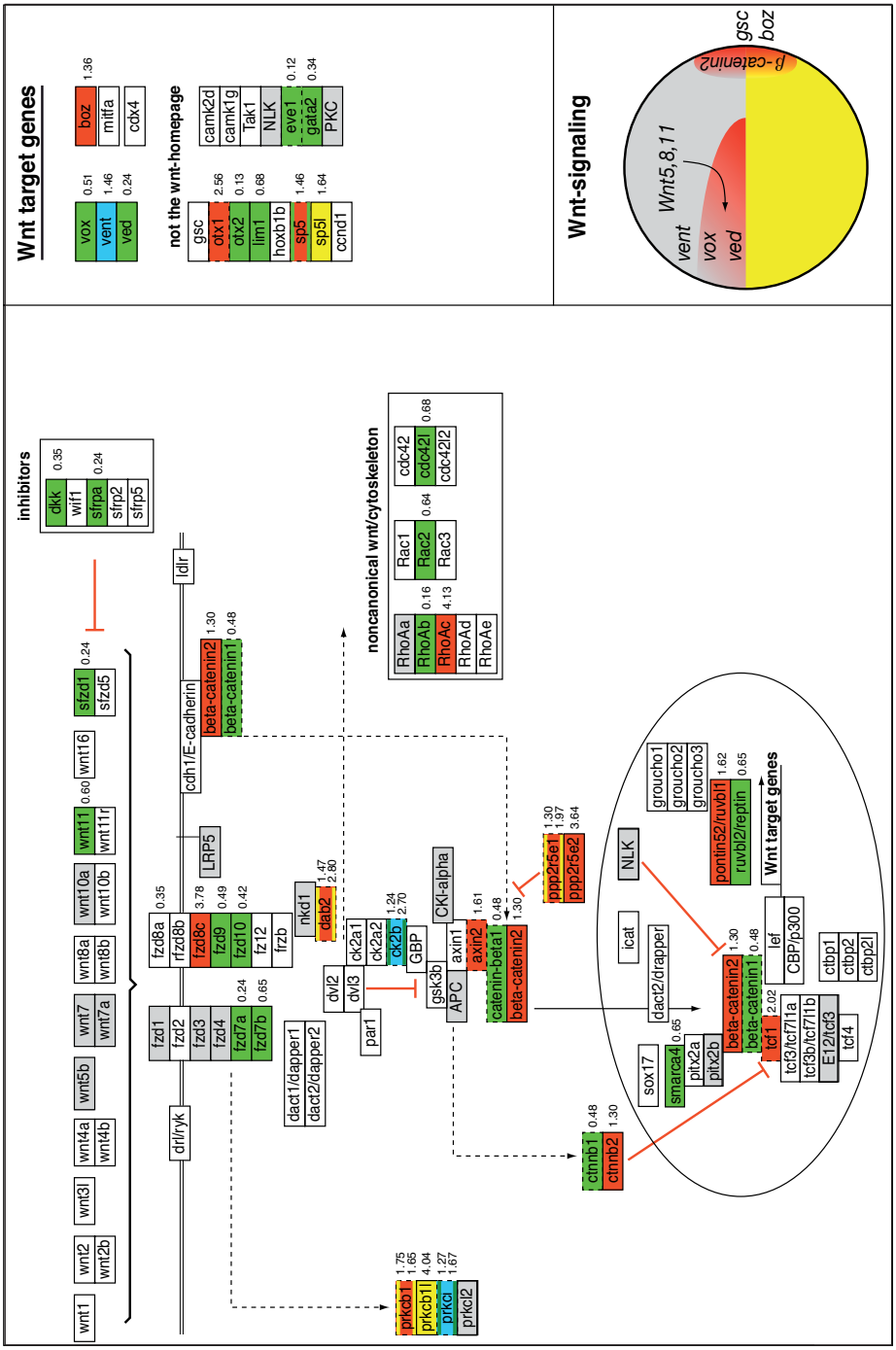
Wnt target genes
vox 0.51
vent 1.46
ved 0.24
boz 1.36
mitfa
cdx4
not the wnt-homepage
gsc
otx1 2.56
otx2 0.13
lim1 0.68
hoxb1b
sp5 1.46
sp5l 1.64
ccnd1
camk2d
camk1g
Tak1
NLK
eve1 0.12
gata2 0.34
PKC
Wnt-signaling
gsc
boz
β-catenin2
Wnt5,8,11
vent
vox
ved
inhibitors
dkk 0.35
wif1
sfrpa 0.24
sfrp2
sfrp5
wnt1
wnt2
wnt2b
wnt3l
wnt4a
wnt4b
wnt5b
wnt7
wnt7a
wnt8a
wnt8b
wnt10a
wnt10b
wnt11 0.60
wnt11r
wnt16
sfzd1 0.24
sfzd5
dtl/ryk
fzd1
fzd2
fzd3
fzd4
fzd7a 0.24
fzd7b 0.65
fzd8a 0.35
rfzd8b
fzd8c 3.78
fzd9 0.49
fzd10 0.42
fz12
frzb
LRP5
idlr
cdh1/E-cadherin
beta-catenin2 1.30
beta-catenin1 0.48
nkd1
dab2 1.47 2.80
dact1/dapper1
dact2/dapper2
dvl2
dvl3
par1
ck2a1
ck2a2
ck2b 1.24 2.70
GBP
gsk3b
APC
CKI-alpha
axin1
axin2 1.61
catenin-beta1 0.48
beta-catenin2 1.30
noncanonical wnt/cytoskeleton
RhoAa
RhoAb 0.16
RhoAc 4.13
RhoAd
RhoAe
Rac1
Rac2 0.64
Rac3
cdc42
cdc42l 0.68
cdc42l2
ppp2r5e1 1.30 1.37
ppp2r5e2 3.64
prkcb1 1.75 1.65
prkcb1l 4.04
prkci 1.27 1.67
prkcl2
ctnnb1 0.48
ctnnb2 1.30
NLK
icat
dact2/dapper
sox17
smarca4 0.65
pitx2a
pitx2b
groucho1
groucho2
groucho3
pontin52/ruvbl1 1.62
ruvbl2/reptin 0.65
Wnt target genes
beta-catenin2 1.30
beta-catenin1 0.48
tcf1 2.02
lef
CBP/p300
tcf3/tcf7l1a
tcf3b/tcf7l1b
E12/tcf3
tcf4
ctbp1
ctbp2
ctbp2l

Figure 6C

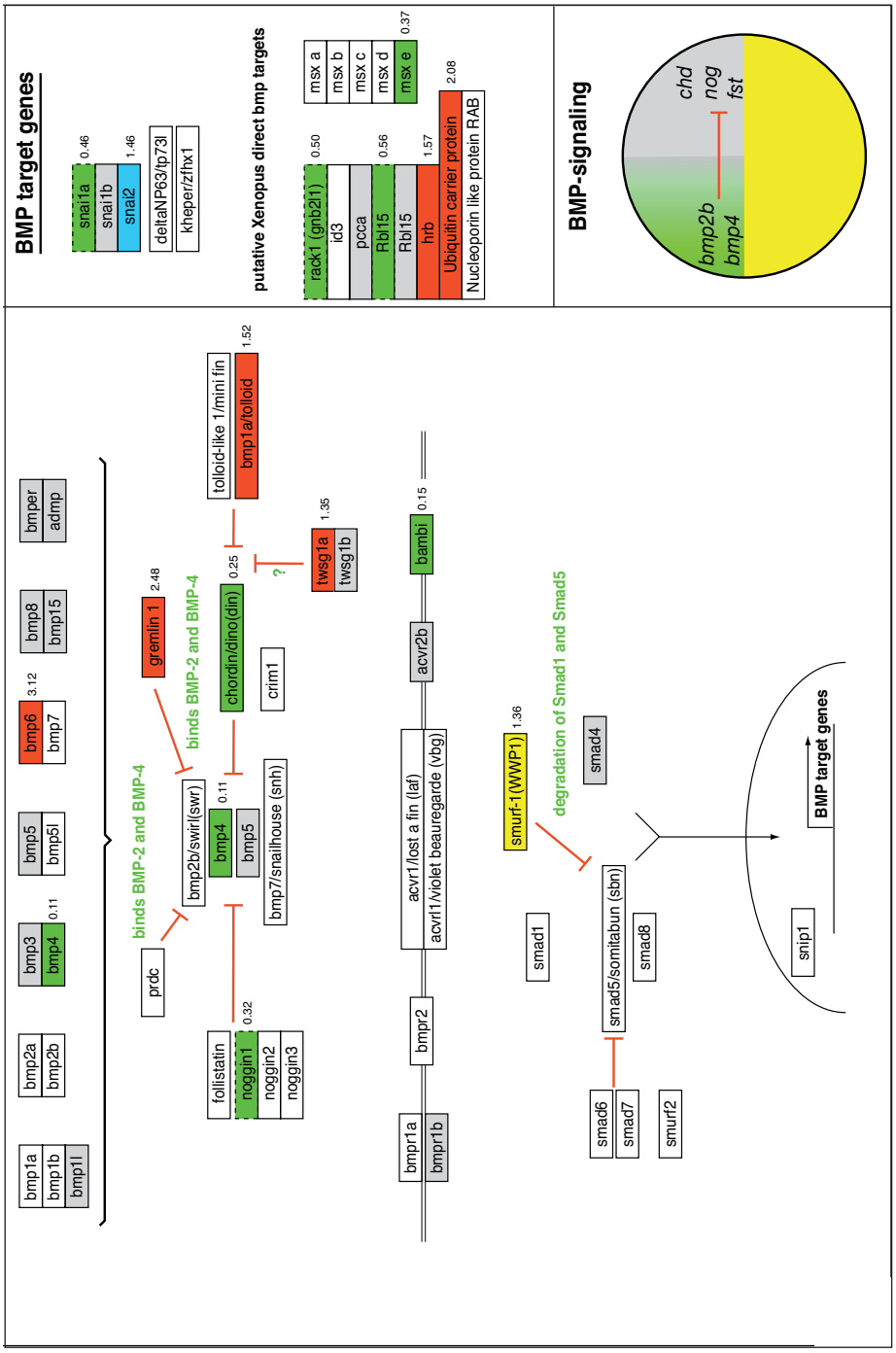
BMP target genes
snai1a
snai1b
snai2
deltaNP63/tp73l
kheper/zfhx1
0.46
1.46
putative Xenopus direct bmp targets
rack1 (gnb2l1)
id3
pcca
Rbl15
Rbl15
hrb
Ubiquitin carrier protein
Nucleoporin like protein RAB
msx a
msx b
msx c
msx d
msx e
0.50
0.56
1.57
2.08
0.37
BMP-signaling
chd
nog
fst
bmp2b
bmp4
bmp1a
bmp1b
bmp1l
bmp2a
bmp2b
bmp3
bmp4
bmp5
bmp5l
bmp6
bmp7
bmp8
bmp15
bmper
admp
0.11
3.12
binds BMP-2 and BMP-4
prdc
bmp2b/swirl(swr)
bmp4
bmp5
bmp7/snailhouse (snh)
0.11
follistatin
noggin1
noggin2
noggin3
0.32
gremlin 1
2.48
binds BMP-2 and BMP-4
chordin/dino(din)
crim1
0.25
tolloid-like 1/mini fin
bmp1a/tolloid
1.52
?
twsg1a
twsg1b
1.35
bmpr1a
bmpr1b
bmpr2
acvr1/lost a fin (laf)
acvrl1/violet beauregarde (vbg)
acvr2b
bambi
0.15
smurf-1(WWP1)
1.36
degradation of Smad1 and Smad5
smad1
smad4
smad5/somitabun (sbn)
smad8
smad6
smad7
smurf2
snip1
BMP target genes

Figure 6D

ity against Nodal, another member of the TGF-beta super-family. Expression starts at blastula stage, immediately after initiation of zygotic transcription, and is localized in the whole blastula margin at late blastula – 30% epiboly stage (Thisse et al., 1999). In ERK1 knockdown embryos, *lft1* expression was up-regulated (+2.54 fold) and down-regulated in ERK2 morphants (-3.27 fold), as also shown in Fig.6A. Whole mount in situ hybridization with *lefty1* probe (Fig.7D-F) at 30% epiboly shows a possible increase of *lefty1* expression in ERK1 morphants (Fig.7E), but the decrease of expression in ERK2 morphants (Fig.7F) was clearly visible.

The T-box gene *notail* (*ntl*) is involved in mesoderm development, as described in the legend to figure 8. At 30% epiboly *ntl* is expressed in the blastula margin (Schulte-Merker S., et al., 1992). This expression is synergistically regulated by FGF and Nodal signaling pathways (Draper et al., 2003; Griffin and Kimelman, 2003). Both of these pathways show a negative regulation in the ERK2 morphants, as shown by the GenMAPP analysis (Fig.6). The negative effect on these pathways and the array-data itself suggested a down-regulation of the *ntl*-gene upon ERK2 knockdown. The expression signatures from the ERK1 and ERK2 morphants revealed that *ntl* expression was not significantly changed in ERK1 morphants (p-value > 10^{-5}), but was down-regulated (-3 fold) in ERK2 morphants. This decrease in expression of *ntl* was also confirmed by whole mount in situ experiments (Fig.7G-I). The *ntl* gene expression in ERK1 morphants was comparable to expression in wild type embryos, but *ntl* expression was decreased in ERK2 morphants. Strikingly, expression of *ntl*

Figure 6. Analysis of developmental signaling processes ERK1MO and ERK2MO gene expression profiles indicate defects in early developmental signaling processes.

(A) Nodal, (B) FGF, (C) canonical Wnt and (D) BMP signaling pathways are overlaid with gene-expression color criterion and ratios of gene-expression from the program GenMAPP: yellow = up-regulated by ERK1MO (ratio > 1), blue = down-regulated by ERK1MO (ratio <1), red = up-regulated by ERK2MO (ratio > 1), green = down-regulated by ERK2MO (ratio <1), gray = gene is not present on the Agilent zebrafish 22k microarrays or in the GenMAPP database, white = not significantly changed.

The genes that were affected in their expression in both ERK1 and ERK2 morphants show multicolored gene-boxes with the expression ratios for both conditions depicted on the right of the gene; the ration for ERK1 knockdown at the top and ERK2 knockdown below. At the right side of the subfigure a list of responsive target-genes is listed for each signaling pathway. The bottom right of each subfigure shows a small representation of the predicted signaling activity in the wild type embryos, based on the potential range of signals and the expression patterns and range of antagonists adopted from Schier and Talbot (2005), late blastula stage, lateral view, dorsal to right and animal pole to top.

was not constant in the marginal ring, as stronger expression was detected in the putative dorsal side of the ERK2 morphants.

The obtained results by whole mount in situ hybridization using *gsc*, *lft1* and *ntl*, confirm the predictions made by the GenMAPP analysis, as the changes in their expression levels are conform the predictions obtained by the signaling pathway analysis of the microarray data.

Discussion

In this study we have performed an expression profiling analysis that gives new mechanistic insights in how ERK signaling is functioning and how it integrates with other known effectors of vertebrate embryogenesis. This expression profiling study compared ERK1 and ERK2 knockdown at late blastula stage revealing different gene expression signature sets and downstream targets for these proteins. The gene expression signatures of ERK1 and ERK2 knockdown were used to obtain new insights in the embryonic processes that were perturbed and to indicate potential downstream target genes that were specifically affected by the knockdown of either ERK1 or ERK2.

Comparison of the effects of ERK1 and ERK2 knockdown

Comparison of the gene expression profiles of the ERK1 and ERK2 morphants with standard control MO injected embryos as a shared reference showed specific gene expression profiles, as different number of genes and different gene pools were found. The gene expression signature sets included genes involved in cell cycle, proliferation, cell differentiation, metabolism, cytoskeleton dynamics, signal transduction, migration and transcription. The gene expression profiles of ERK1 and ERK2 and knockdown embryos showed a set of genes that were commonly regulated (Fig.2B). Surprisingly, we also found a set of genes that was regulated in an anti-correlated manner. This observation is in line with the notion that ERK1 and ERK2 have specific down stream targets.

The higher number of genes affected by the knockdown of ERK2 is in agreement with the severe phenotype of ERK2 knockdown embryos. In order to understand the severe effects of ERK1/2 knockdown, we have to consider the results in the context of the known signaling pathways that govern developmental programs as proliferation, cell migration and differentiation processes. Therefore we performed signaling pathway analysis on the ERK1 and ERK2 transcriptome signatures using the GenMAPP software program for analysis of

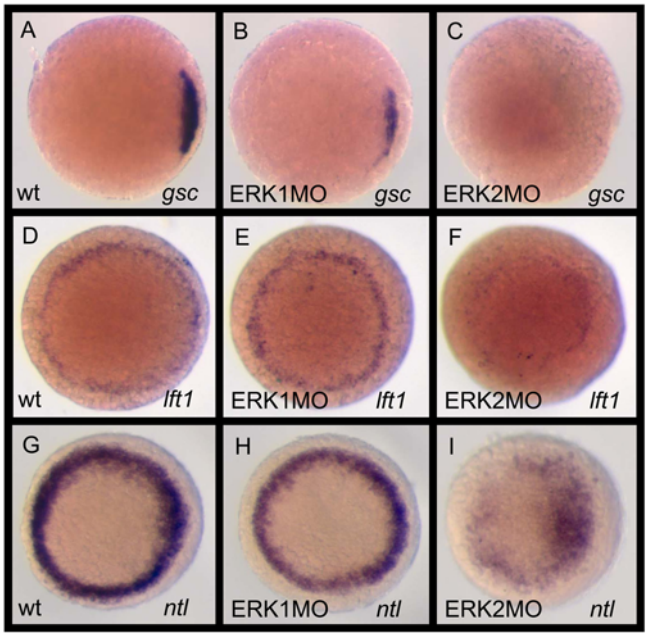

Figure 7. Effects of ERK1 and ERK2 knockdown are confirmed by whole mount in situ hybridization. The zebrafish embryos were injected with 3.4ng ERK1MO (B,E,H) or ERK2MO (C,F,I) and in situ expression patterns were compared to wild type embryos (A,D,G). The embryos were fixed at 4.5hpf, processed for whole mount in situ hybridization, and imaged (animal pole view, dorsal to right). A,B,C: *goosecoid* (*gsc*, presumptive shield/dorsal organizer); D,E,F: *lft1*/*antivin* (blastula margin); G,H,I: *notail* (*ntl*, blastula margin)

important signaling pathways involved in early vertebrate development. These include the Nodal, FGF, Wnt and BMP signaling pathways.

ERK1 and ERK2 are involved in different developmental processes

For biological interpretation of the obtained expression profiles, analysis of gene ontology (GO) can be used as a tool to indicate processes that are likely to be affected. Different gene ontology clusters showed a relative enrichment in ERK1 versus ERK2 knockdown gene expression signatures. Since the annotation of the zebrafish genome is the limiting factor in assigning biological functions we have focused on gene onthologies that are relatively well known and have further supported the analyses by manual annotation of our signa-

ture sets. For instance, this leads to the conclusion that the biological GO-clusters 'development' was significant under-represented for both ERK1 and ERK2 knockdown. More detailed analysis was performed using the signaling-pathway based GenMAPP gene map annotator and pathway profiler program. This led to a model for the distinct effects of ERK1 and ERK2 knockdown in developmental signaling processes as summarized in figure 8. Early embryo developmental processes include mesoderm formation, endoderm formation dorsal-ventral pattering, anterior-posterior patterning and gastrulation movements. To establish a mesodermal zone, next to the dorsal-ventral patterning, also induction processes occur at the animal-vegetal axis. Complex signaling processes are used by the embryo to induce mesoderm, as nicely reviewed by Kimelman (Nature reviews 2006). Based on literature data it is possible to interpret the observed expression patterns and knockdown effects in the context of known signaling pathways underlying these processes as described in the legend to figure 8.

Under the milder knockdown conditions used in chapter 4, reduced expression of ventral markers and concomitant expansion of dorsal marker-genes was found. However, these changes in patterning were not considered sufficient evidence to conclude an altered cell specification. The use of more stringent knockdown conditions as applied in this array-based study showed that in ERK1 morphants the ventrally expressed patterning gene *vent* was down-regulated, but also the BMP inhibitory gene *smurf1* was up-regulated, possibly responsible for inhibition of BMP signaling on the ventral side (Fig. 8, panel D and B). This may lead to a dorsalization of ERK1 knockdown embryos. Surviving ERK1 morphants showed a tailless phenotype (data not shown / chapter 4). This supports a block of BMP-signaling, as tail formation is combinatory regulated by BMP and FGF signaling since mutant embryos for *bmp2b* fail to form tails (Agathon et al., 2003) and embryos with impaired FGF-signaling show tailless phenotypes. However, it is important to note that also genes involved in regulating gastrulation cell migration were altered in expression (*oep* and *quattro*) (Hammerschmidt et al., 2003; Dagget et al., 2004). This makes it difficult to determine whether ERK1 morphants show affected convergence cell migration, due to altered patterning and cell fate specification or due to cell migratory events as described in chapter 4 using less stringent knockdown conditions.

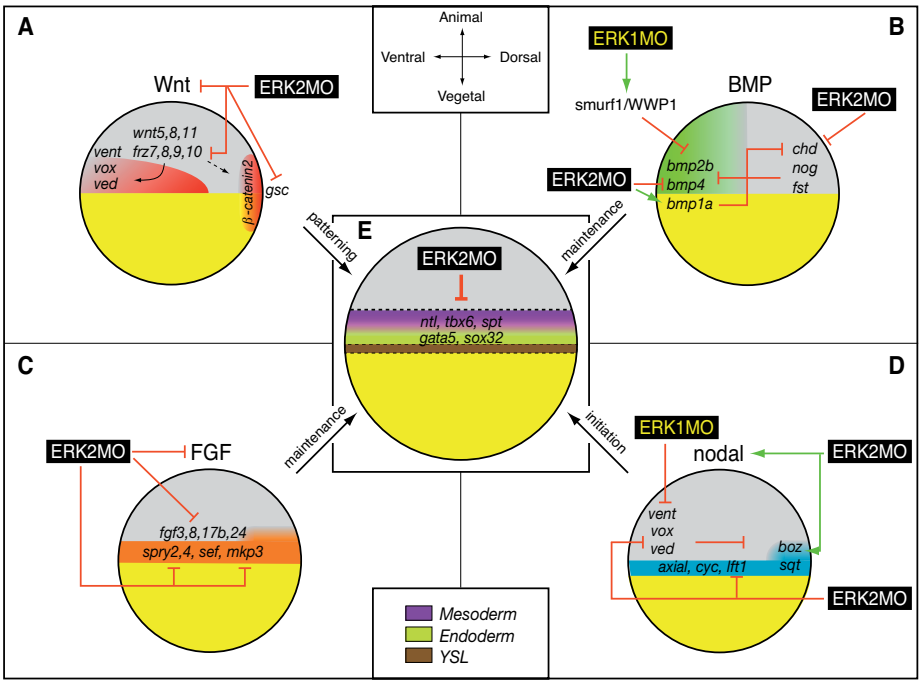

Figure 8. ERK1 and ERK2 knockdown differently affect signals involved in patterning of the early embryo. (A-D): Schematic representation of the effects of ERK1 and ERK2 knockdown on the activities of Nodal, FGF, Wnt and BMP signaling pathways in late blastula embryos. (E): effect of ERK2 knockdown (ERK2MO) on early embryonic mesendoderm differentiation. The representation of predicted signaling activity in the wild type embryos is based on the potential range of signals, the expression patterns and range of antagonists, adopted from Schier and Talbot (2005). The combined signaling activities from these pathways are responsible for the differentiation and fate-map of the late blastula/early gastrula stage of the zebrafish embryo (E, late blastula stage, lateral view, dorsal to right, animal pole to top). In the zebrafish embryo, dorsal ventral patterning starts as early as the 128-cell stages by accumulation of β-catenenin at the nuclei of the dorsal cells, rapidly followed by the expression of *goosecoid* (A). Soon after mid-blastula transition, β-catenin also activates the expression of a number of zygotic genes, including *chordin*, *bozozok* and *squint* (A and D), and FGF signals (C). These genes act to inhibit the action of ventralizing factors or induce mesoderm and endoderm cell fates at the dorsal side. Subsequently, the expression of these genes quickly spreads over the complete margin (panel E). To establish a mesodermal zone induction processes occur at the animal-vegetal axis. Complex signaling processes are used by the embryo to induce mesoderm. In a over-simplified manner, it can be said that Nodal (D) signaling is involved in initiation of mesoderm formation, FGFs (C) and Wnt (A) are involved in maintaining the mesoderm state and BMPs (B) are involved in further patterning of the mesoderm (Kimelman, 2006).

Figure 8. continued: Knockdown of ERK1 (ERK1MO) resulted in an increased expression of the BMP-inhibiting protein *smurf1*/*wwp1* and the ventrally expresses gene *vent* (A). Combined, this indicates a reduction of ventral signaling, possibly leading to a dorsalization of the embryo. ERK2 knockdown (ERK2MO) promotes Nodal signaling by repressing the expression of Nodal inhibitors (*vox*, *ved*, *lft1*) (D). Furthermore, it perturbs FGF signaling (repression of *fgf8* and components of the RAS-ERK pathway and down regulation of its target genes) and Wnt signaling (repressed expression of frizzled receptors and key components of the Wnt pathway). In addition, perturbed BMP signaling results in incorrect patterning of the mesoderm (B). In summary, this shows that mesendoderm differentiation is still initiated by Nodal signaling (D), but mesendoderm maintenance by FGF and Wnt signaling is defected. This results in reduced expression of mesoderm (*ntl*, *tbx6* and *spt*) and endoderm (*gata5*, *sox32*) marker genes (B, C and E), showing that ERK2 is essential for mesendoderm differentiation (E).

ERK2 signaling is essential for the maintenance of the mesendodermal cell fates

In ERK2 morphants no active MAPK was detected at the margin at 4.5hpf (chapter 4) suggesting that Ras-Raf-MEK-ERK dependent FGF signaling and subsequent downstream signaling was blocked. FGF signaling acts as a competence factor for cells to respond to Nodal mediated mesoderm induction. As our data shows that ERK2 morphants are severely impaired in both FGF and Wnt signaling it is likely that mesoderm progenitor cells in the margin are affected in the maintenance of the mesodermal cell fates (Fig.8E). However, it has been reported that Nodal and FGF pathways interact through a positive regulatory loop and synergize to maintain mesodermal cell populations (Mathieu et al., 2004), in addition FGF signaling negatively regulates Nodal-dependent endoderm induction in zebrafish (Mizoguchi et al., 2006). This would suggest that Nodal-mediated initation of mesoderm differentiation is still present, but the maintenance of the mesoderm, mediated by FGF and Wnt, is affected.

In *Drosophila*, FGF-dependent ERK activation was shown to be required for proper mesoderm dispersal (Gabay et al.,1997; Gryzik and Muller, 2004; Stathopoulos et al., 2004). In *Xenopus*, ERK2 was shown to be required for mesoderm differentiation (Gotoh et al., 1995). Mouse *erk2*-/- embryos also fail to form mesoderm at E6.5 and E7.5 based on histological criteria, but *erk2*-/- embryonic stem cells were still capable of forming mesoderm. However, treatment of these ES cells with the MAPK inhibitor PD184352 decreased total ERK activity in these cells and expression of the mesoderm marker *brachyury*/*ntl* (essential for posterior mesoderm and axis formation) (Yao et al., 2003). Our gene expression profiling shows that ERK2 plays a role in mesoderm development based on additional mesoderm markers (e.g. *spt*/*tbx16*, *tbx6*), but

importantly also by addressing the upstream signaling mechanisms involved in mesoderm initiation and maintenance. It should be noted that ERK-activation is not only mediated by FGF signaling, but also influenced by other growth factors (PDGF, VEGF), G-protein coupled receptor signaling and hormone- and Ca^{2+} signaling pathways. A nice example that shows the complexity of interconnections, redundancy and crosstalk between the different pathways is the work of Poulain et al. (2006), showing that combinatorial Nodal, FGF and BMP signaling regulates endoderm formation in zebrafish. The authors also show that activation of FGF-signaling or injection of constitutive active (rat) ERK2 lead to phosphorylation of Sox32 and repression of the endoderm marker *sox17*. However, in our study, ERK2 morphants showed a reduced expression of the upstream Nodal responsive genes *gata5*, *sox32* and *sox17*. These genes are normally expressed in presumptive endoderm progenitor cells in the margin at 4.5 hpf (Aoki et al.,2002). This suggests that depletion of ERK2 also affects endoderm differentiation (Fig.8). Follow-up experiments, using different times of development in combination with chromatin immunoprecipitation (chIP-chip) methodology will be needed to further understand the crucial function of ERK2 in mesendoderm development and determine specific target genes.

Conclusions

Our analysis of the gene expression microarray data revealed that ERK1 and ERK2 knockdown affected a set of common, as well as specific downstream genes. Surprisingly we also discovered a set of genes with anti-correlated expression. The gene ontology analyses show that ERK1 and ERK2 have specific roles in embryogenesis and target distinct gene sets involved in vertebrate development, confirming the embryonic knockdown phenotypes. The signaling pathway analysis on the ERK1 and ERK2 transcriptome signatures using the GenMAPP software program for analysis of BMP, FGF, Nodal and Wnt signaling pathways showed distinct roles for these MAP kinases. For ERK1 knockdown we identified a connection with genes involved in dorsal-ventral patterning and subsequent embryonic cell migration. For ERK2 knockdown we identified a connection with genes involved in mesoderm and endoderm initiation, differentiation and patterning. The outcome of the predictions for ERK2 knockdown on developmental signaling were confirmed by the observed effects on mesoderm and endoderm patterning and subsequent whole mount in situ hybridization experiments. Our results show the strength of gene expression profiling of morpholino knockdown embryos in combination with versatile bioinformatics tools.

Experimental procedures

Zebrafish Morpholino knockdown experiments

Zebrafish embryos were injected at the one-cell stage 1 nl of the solubilized compounds in 1× Danieau's buffer [58 mM NaCl, 0.7 mM KCl, 0.4 mM $MgSO_4$, 0.6 mM $Ca(NO_3)_2$, 5.0 mM HEPES; pH 7.6] containing 1% Phenol red solution (Sigma). Definition of stages was according to Kimmel et al. at 1K-stage (3hpf), embryos with a red animal pole were selected as positive-injected embryos.

To block translation of the ERK1 or ERK2 protein, 0.4mM (3.4ng) morpholinos (MOs) were injected per embryo. MOs were targeted against the 5'-UTR of the respective mRNAs (GeneTools Philomath, OR, USA): ERK1-MO, 5'-TCTGTCCGCAAATCGTCGCCTTCGC; ERK2-MO, 5'-CACCCAAAAGCACCAGGAAAAGCTC. As a control, the standard control MO 5'-CCTCTTACCTCAGTTACAATTTATA was used at the same concentration. Injected embryos were kept at 28°C until desired stages, until sacrifice.

RNA isolation from zebrafish embryos

The zebrafish embryos were homogenized in liquid nitrogen and total RNA was extracted using Trizol reagent (Invitrogen) according to the manufacturer's instructions. To remove genomic DNA, RNA samples were incubated at 37°C for 15 min with 10 units of DNaseI (Roche). The RNA samples were purified using the RNeasy kit (Qiagen) according to the RNA Cleanup protocol. Total RNA concentrations were determined spectrophotometrically using a Nanodrop ND-1000 (Isogen Life science). Optical density A260/A280 ratios of all samples ranged from 1.8-1.9, indicating high purity.

Experimental design, Labeling and Hybridization of Agilent 22K-microarrays

A total of 7 Agilent 22K-microarray hybridizations were performed for this experiment. 2 independent biological replicates were analyzed for each gene and in the case of ERK2, at least an additional technical replicate were hybridized for each biological replicate, including 2 dye swaps. For each biological sample, a number of 70-100 morpholino injected embryos were collected at 30% epiboly stage. The RNA from standard control MO injected embryos was labeled with Cy3 and those of ERK1MO and ERK2MO injected embryos were labeled with Cy5, using the Agilent Low RNA Input Linear Amplification kit. Hybridization and scanning were performed by Service XS (Leiden, the Netherlands).

Data analysis of Agilent 22K-microarrays

Feature extraction also performed by Service XS using Agilent FE 8.5 software; all subsequent analysis were performed using the default settings implemented in Rosetta Resolver v 6.0 for an error modeling-based normalization.

For the analysis and detailed annotation shown in the Venn diagrams and tables, we focused on the genes that were most significantly affected. For that selection we used the following criteria: the absolute fold change should be at least 1.5 in each independent replicate; and the p-value provided by the error-model taking into account all hybridizations combined must be smaller than 10^{-5} to compensate for multiple testing false positives. For the tables used for GenMAPP (www.genmapp.org) analysis we took a less stringent approach not limiting the number of genes by fold change, therefore using all genes that had a combined p-value smaller than 10^{-5}.

cDNA synthesis and Quantitative PCR

cDNA synthesis was performed using a TGradient Thermocycler 96 (Whatman Biometra) according to the manufacturer's instructions. RNA samples were identical to those used for microarray hybridization. Reactions were performed in a 20 µl mixture of 150 ng RNA, 4 µl of 5x iScript Reaction mix (Bio-Rad) and 1 µl of iScript Reverse Transcriptase (Bio-Rad). The reaction mixtures were incubated at 25 °C for 5 min, 42 °C for 30 min, and 85 °C for 5 min.

Quantitative real-time PCR was performed using the Chromo4 Four-color Real-time PCR detection system (Bio-Rad laboratories, Hercules, CA) according to the manufacturers' instructions. Gene-specific primers for quantitative real-time PCR were designed, using Beacon Designer software, to generate single gene-specific amplicons of 75-150 nucleotides. Reactions were performed in a 25 µl volume comprised of 1 µl cDNA, 12.5 µl of 2x iQ SYBR Green Supermix (Bio-Rad) and 10 pmol of each primer. Cycling parameters were 94 °C for 3 min to activate the polymerase, followed by 40 cycles of 94 °C for 15 sec and 59 °C for 45 sec. Fluorescence measurements were taken at the end of each cycle. Melting curve analysis was performed to verify that no primer dimers were amplified. All reactions were done in duplicate or triplicate and the threshold cycle C_T values were plotted against the base 10 log of the amount of cDNA by using Opticon Monitor 3.1 (Bio-Rad) according to the manufacturer's instructions. For evaluation of PCR efficiencies of all primers sets standard curves were generated using serial diluted cDNA samples (dilution factors of 1, 5, 25, 125 and 625) and strong linear correlations between the C_T values and the log of input cDNA amount were obtained, indicating correla-

tion coefficiencies ranging from 98% to 101%. Data were normalized using the Genex macro provided by Bio-Rad.

The expression level were tested for *mycn (*v-myc, myelocytomatosis viral related oncogene, neuroblastoma derived; NM_212614), *fos* (*v-fos,* FBJ murine osteosarcoma viral oncogene homolog; NM_205569) and mos (v-mos, Moloney murine sarcoma viral oncogene homolog; NM_205580). β-actin was taken as reference and it showed unchanged expression level between standard control MO injected and ERK1MO or ERK2MO injected embryos. Sequences of forward and reverse primers were 5'- CGAGCAGGAGATGGGAACC and 5'- CAACGGAAACGCTCATTGC for β-actin (AF057040); *mycn* (NM_212614) qP1fw GAGGATGATGAGGAAGATGATGAAG, qP2rv CCTGCCTGAGAGTTGGAGAC; *fos* (NM_205569) qP1Fw TGACCTGGAGCCGCTTTGC, and qP2rv GGTAGGTGAACATGAAGGAAGACG; *mos* (NM_205580) qP1fw CCCTCACCAATCCCCGTCAC , and qP2rv GAGCCTGTGTGCGACTTTACC
.

Whole mount in situ hybridization

Embryos were fixed overnight in 4% paraformaldehyde in PBS at 4 °C and in situ hybridization was performed as described previously (Thisse et al., 1993) using described probes for *gsc*, *ntl* and *lft1*/*antivin*.

ACKNOWLEDGEMENTS

We gratefully acknowledge Zoltan Hegedus for the help with the annotation of the complete 22K Agilent zebrafish microarray chips. We thank Carl Philipp Heisenberg for fruitfull discussions and providing us with the *lft1* probe construct. In addition, we thank Annemarie Meijer and Enrique Salas-Vidal for stimulating discussions and their contributions. This work was supported by a European Commission 6th Framework Program grant (contract LSHG-CT-2003-503496, ZF-MODELS).

References

1. Agathon, A., Thisse, C., and Thisse, B. (2003) The molecular nature of the zebrafish tail organizer. Nature, 424, 448-452.
2. Aoki, T.O., David, N.B., Minchiotti, G., Saint-Etienne,L., Dickmeis, T., Persico, G.M., Strahle, U., Mourrain, P., and Rosa,F.M. (2002) Molecular integration of casanova in the Nodal signalling pathway controlling endoderm formation. Development, 129, 275-286.
3. Behrens, J., Jerchow,B.A., Würtele,M., Grimm,J., Asbrand,C., Wirtz,R., hl,M., Wedlich,D., and Birchmeier,W. (1998) Functional Interaction of an Axin Homolog, Conductin, with {beta}-Catenin, APC, and GSK3. Science, 280, 596-599.
4. Beisvag,V., Junge,F., Bergum,H., Jolsum,L., Lydersen,S., Gunther,C.C., Ramampiaro,H., Langaas,M., Sandvik,A., and Laegreid,A. (2006). GeneTools - application for functional annotation and statistical hypothesis testing. BMC Bioinformatics, 7, 470.
5. Bottcher,R.T. and Niehrs,C. (2005) Fibroblast Growth Factor Signaling during Early Vertebrate Development. Endocr Rev, 26, 63-77.
6. Daggett,D.F., Boyd,C.A., Gautier,P., Bryson-Richardson,R.J., Thisse,C., Thisse,B., Amacher,S.L., and Currie,P.D. (2004) Developmentally Restricted Actin-Regulatory Molecules Control Morphogenetic Cell Movements in the Zebrafish Gastrula. Current Biology, 14, 1632-1638.
7. Dahlquist,K.D., Salomonis,N., Vranizan,K., Lawlor,S.C., and Conklin,B.R. (2002) GenMAPP, a new tool for viewing and analyzing microarray data on biological pathways. Nature Genetics, 31, 19-20.
8. Draper,B.W., Stock,D.W., and Kimmel,C.B. (2003). Zebrafish fgf24 functions with fgf8 to promote posterior mesodermal development. Development, 130, 4639-4654.
9. Gabay, L., Seger, R., and Shilo, B.Z. (1997) MAP kinase in situ activation atlas during Drosophila embryogenesis. Development, 124, 3535-3541.
10. Pagès, G., Guérin, S., Grall, D., Bonino, F., Smith, A., Anjuere, F., Auberger, P., and Pouysségur, J., (1999) Defective Thymocyte Maturation in p44 MAP Kinase (Erk 1) Knockout Mice. Science, 286, 1374-1377.
11. Gotoh, Y., Masuyama, N., Suzuki, A., Ueno, N., and Nishida, E. (1995) Involvement of the Map Kinase Cascade in Xenopus Mesoderm Induction. Embo Journal, 14, 2491-2498.
12. Gotoh, Y. and Nishida, E. (1996) Signals for mesoderm induction. Roles of fibroblast growth factor (FGF)/mitogen-activated protein kinase (MAPK) pathway. Biochimica et Biophysica Acta (BBA) - Reviews on Cancer, 1288, F1-F7.
13. Griffin, K.J.P. and Kimelman, D. (2003) Interplay between FGF, one-eyed pinhead, and T-box transcription factors during zebrafish posterior development. Developmental Biology, 264, 456-466.
14. Gryzik, T. and Muller, H.A.J. (2004) FGF8-like1 and FGF8-like2 encode putative ligands of the FGF receptor Htl for mesoderm migration and are required in the Drosophila gastrula. Current Biology, 14, 659-667.
15. Hammerschmidt, M., Pelegri, F., Mullins, M.C., Kane, D.A., Brand, M., vanEeden, F.J.M.,

Furutani Seiki, M., Granato, M., Haffter, P., Heisenberg, C.P., Jiang, Y.J., Kelsh, R.N., Odenthal, J., Warga, R.M., and NussleinVolhard, C. (1996) Mutations affecting morphogenesis during gastrulation and tail formation in the zebrafish, Danio rerio. Development, 123, 143-151.

16. Johnson, G.L., Dohlman, H.G., and Graves, L.M. (2005) MAPK kinase kinases (MKKKs) as a target class for small-molecule inhibition to modulate signaling networks and gene expression. Current Opinion in Chemical Biology, 9, 325-331.
17. Kimelman, D. (2006) Mesoderm induction: from caps to chips. Nature Reviews Genetics, 7, 360-372.
18. Kimmel, C.B., Ballard, W.W., Kimmel, S.R., Ullmann, B., and Schilling, T.F. (1995) Stages of Embryonic-Development of the Zebrafish. Developmental Dynamics, 203, 253-310.
19. Lloyd, A. (2006) Distinct functions for ERKs? Journal of Biology, 5, 13.
20. Maegawa, S., Varga, M., and Weinberg, E.S. (2006) FGF signaling is required for {beta}-catenin-mediated induction of the zebrafish organizer. Development, 133, 3265-3276.
21. Mathieu, J., Griffin, K., Herbomel, P., Dickmeis, T., Strahle, U., Kimelman, D., Rosa, F.M., and Peyrieras, N. (2004) Nodal and Fgf pathways interact through a positive regulatory loop and synergize to maintain mesodermal cell populations. Development, 131, 629-641.
22. Melby, A.E., Beach, C., Mullins, M., and Kimelman, D. (2000) Patterning the Early Zebrafish by the Opposing Actions of bozozok and vox/vent. Developmental Biology, 224, 275-285.
23. Mizoguchi, T., Izawa, T., Kuroiwa, A., and Kikuchi, Y. (2006) Fgf signaling negatively regulates Nodal-dependent endoderm induction in zebrafish. Developmental Biology, 300, 612-622.
24. Nasevicius, A. and Ekker, S.C. (2000) Effective targeted gene ‘knockdown’ in zebrafish. Nat Genet, 26, 216-220.
25. Saba-El-Leil, M.K., Vella, F.D.J., Vernay, B., Voisin, L., Chen, L., Labrecque, N., Ang, S.L., and Meloche, S. (2003) An essential function of the mitogen-activated protein kinase Erk2 in mouse trophoblast development. Embo Reports, 4, 964-968.
26. Schier A.F., Talbot. W. S. (2005) Molecular genetics of axis formation in zebrafish. Annu Rev Genet. 39, 561-613.
27. Schulte-Merker, S., Ho, R.K., Herrmann, B.G., and Nusslein-Volhard, C. (1992) The protein product of the zebrafish homologue of the mouse T gene is expressed in nuclei of the germ ring and the notochord of the early embryo. Development, 116, 1021-1032.
28. Stachel, S.E., Grunwald, D.J., and Myers, P.Z. (1993) Lithium perturbation and goosecoid expression identify a dorsal specification pathway in the pregastrula zebrafish. Development, 117, 1261-1274.
29. Stathopoulos, A., Tam, B., Ronshaugen, M., Frasch, M., and Levine, M. (2004) pyramus and thisbe: FGF genes that pattern the mesoderm of Drosophila embryos. Genes and Development, 18, 687-699.
30. Thisse, C. and Thisse, B. (1999) Antivin, a novel and divergent member of the TGFbeta

superfamily, negatively regulates mesoderm induction. Development, 126, 229-240.

31. Thisse, C., Thisse, B., Schilling, T.F., and Postlethwait, J.H. (1993) Structure of the zebrafish snail1 gene and its expression in wild-type, spadetail and no tail mutant embryos. Development, 119, 1203-1215.
32. Vantaggiato, C., Formentini, I., Bondanza, A., Bonini, C., Naldini, L., and Brambilla, R. (2006) ERK1 and ERK2 mitogen-activated protein kinases affect Ras-dependent cell signaling differentially. Journal of Biology 5 [5], 14.1-14.15.
33. Warga, R.M. and Kane, D.A. (2003) One-eyed pinhead regulates cell motility independent of Squint/Cyclops signaling. Developmental Biology, 261, 391-411.
34. Yao, Y., Li, W., Wu, J., Germann, U.A., Su, M.S.S., Kuida, K., and Boucher, D.M. (2003) Extracellular signal-regulated kinase 2 is necessary for mesoderm differentiation. PNAS, 100, 12759-12764.

Supplementary data

The following supplemental data files can be found online at;
http://biology.leidenuniv.nl/~krens

Table S1. *Anti-correlated genes1: ERK1MO up-regulated, ERK2MO down-regulated*
The genes with an unigene-IDs flagged with an asterisk (*) = were also found in one of the microarray experiment where standard control MO injected embryos were tested versus control-injection (phenol red), with an absolute fold change of 1.5 and a p-value smaller than 10^{-5}

Table S2. *Anti-correlated genes2: ERK1MO down-regulated, ERK2MO up-regulated*
The genes with an unigene-IDs flagged with an asterisk (*) = were also found in one of the microarray experiment where standard control MO injected embryos were tested versus control-injection (phenol red), with an absolute fold change of 1.5 and a p-value smaller than 10^{-5}.

Table S3. *Common down-regulated genes by ERK1MO and ERK2MO*

Table S4. *Common up-regulated genes by ERK1MO and ERK2MO*

Table S5. *ERK1MO specific genes at 4hpf (30% epiboly)*
The ERK1MO specific genes were selected according to the following stringent filter: the fold change must have been 1.5 fold in each individual experiment and the combined p-value must be 10^{-5}.

Table S6. *ERK2MO specific genes at 4hpf (arrested)*
(1.5 fold in each individual experiment, combined p-value = 10^{-5})

Table S7. *Common effected genes by ERK1MO, ERK2MO and CTRMO*
(combined p-value = 10^{-5})